

Morphology of Luminous Infrared Galaxies in the Local Universe

J. L. Wang^{1,2,3}, X. Y. Xia³, S. Mao^{4,3}, C. Cao^{1,2}, Hong Wu¹, Z. G. Deng⁵

ABSTRACT

We study the morphology, stellar mass and star formation rate of 159 local luminous infrared galaxies (LIRGs) using multi-color images from Data Release 2 (DR2) of the Sloan Digital Sky Survey (SDSS). The LIRGs are selected from a cross-correlation analysis between the *IRAS* survey and SDSS. They are all brighter than 15.9 mag in the *r*-band and below redshift ~ 0.1 , and can be reliably classified morphologically. The fractions of interacting/merging and normal disk galaxies are 48% and 40% respectively. The normal disk galaxies tend to have lower infrared luminosity than interacting/merging galaxies and hence become an increasingly important population at lower infrared luminosity. Our results complement and confirm the morphology evolution trend of LIRGs found by Melbourne, Koo & Le Floc'h (2005) from $z \sim 1$ to $z \sim 0.1$. We also find that about 75% of disk galaxies in the local LIRGs are barred, indicating that bars play an important role in triggering star formation rates $\gtrsim 20 M_{\odot} \text{ yr}^{-1}$ in the local universe.

Subject headings: galaxies : formation - infrared: galaxies - galaxies: interactions - galaxies: starburst - galaxies - spiral

1. INTRODUCTION

Ultraluminous infrared galaxies (ULIRGs) are a class of star forming galaxies discovered by the InfraRed Astronomical Satellite (*IRAS*). Studies have convincingly established that they are interacting/merging galaxies with massive starbursts (see, e.g., Sanders & Mirabel

¹National Astronomical Observatories, Chinese Academy of Sciences, A20 Datun Road, 100012 Beijing, China; Email: wjianl@bao.ac.cn.

²Graduate School of the Chinese Academy of Sciences, 100039 Beijing, China.

³Dept. of Physics, Tianjin Normal University, 300074 Tianjin, China.

⁴Jodrell Bank Observatory, University of Manchester, Macclesfield, Cheshire SK11 9DL, UK.

⁵College of Physical Science, Graduate School of the Chinese Academy of Sciences, 100049 Beijing, China.

1996 and Lonsdale et al. 2006 for reviews; Cui et al. 2002), and may eventually form sub- L^* early type galaxies in the local universe (Genzel et al. 2001). Massive submillimeter emitting galaxies, uncovered by deep SCUBA surveys on blank fields, resemble scaled-up versions of the local ultraluminous infrared galaxies at high redshift, but they may be massive galaxies in formation at high- z (e.g. Tacconi et al. 2006).

Recently, the luminous infrared galaxies (LIRGs, with $10^{11}L_\odot < L_{\text{IR}} < 10^{12}L_\odot$) with an average star formation rate of $\sim 100 M_\odot \text{ yr}^{-1}$ have attracted as much attention as ULIRGs, especially after the launch of *Spitzer Space Telescope* (Werner et al. 2004). It is well known that the star formation density steeply declines from $z \sim 1$ to 0, but the precise reason for this rapid decline is still a matter of debate (e.g. Hammer et al. 2005; Le Floc'h et al. 2005). From the spectral energy distributions of galaxies, Dickinson et al. (2003) predict that 30% to 50% of the stellar mass in present-day galaxies has been formed since $z \sim 1$. Since massive early type galaxies have already been assembled before $z \sim 1$ (e.g. Cowie et al. 1996; Hammer et al. 2005), most of the stellar mass assembly since $z \sim 1$ should occur in intermediate-mass galaxies with mass between $\text{few} \times 10^{10}M_\odot$ to $\text{few} \times 10^{11}M_\odot$, and hence the decline of the star formation activities should occur in such galaxies as well. In fact, Elbaz (2005) found, based on an ISO deep survey, that the IR emission of galaxies rapidly decreases from $z \sim 1$ to $z=0$ and the comoving infrared luminosity by LIRGs is about several tens times larger at $z \sim 1$ than today. *Spitzer* observations of the Chandra Deep Field South (CDFS) confirm the rapid decline of the comoving infrared luminosity density and the number density of LIRGs since $z \sim 1$ (Le Floc'h et al. 2005). It is important to investigate how the properties of LIRGs evolve in order to understand the decline of the star formation density since $z \sim 1$.

Zheng et al. (2004) studied the morphologies of 36 distant LIRGs ($0.4 < z < 1.2$) with HST images. They find that only 17% LIRGs are obvious mergers and the fraction of interacting/merging systems is at most 58%. Furthermore, $\sim 36\%$ distant LIRGs are classified as normal disk galaxies and $\sim 25\%$ are compact sources. The average stellar mass of LIRGs is $\sim 10^{11}M_\odot$. Therefore it is likely that a large fraction of distant LIRGs are star forming disk galaxies through various morphological phases at intermediate redshift, and a substantial fraction of the stellar mass in disk galaxies may be assembled through an LIRG phase since redshift 1. Although the sample size of Zheng et al. (2004) is small, subsequent works based on larger samples arrived at similar classification conclusions. For example, Bell et al. (2005) investigated several hundred infrared luminous galaxies with $5 \times 10^{10}L_\odot < L_{\text{IR}} < 3 \times 10^{11}L_\odot$ at $z \sim 0.7$ in CDFS and find that more than half of $z \sim 0.7$ infrared luminous galaxies are massive spirals with stellar mass larger than $\sim 10^{10}M_\odot$ and less than a third are strongly interacting/merging galaxies. The most comprehensive study on the morphological evolution of LIRGs since $z \sim 1$ is by Melbourne et al. (2005) based on 119 LIRGs in the

Great Observatories Origins Deep Survey-North field (GOODS-N) with the redshift range of $z \sim 0.1$ to 1. For this LIRG sample, the optical morphologies and photometries are from HST, redshifts are from Keck observations, while the infrared luminosities are obtained from *Spitzer*. They also find evidence for the morphological evolution for LIRGs in the last ~ 8 Gyr. Above $z=0.5$, about half of LIRGs are spirals and the ratio of peculiar/irregular to spiral is about 0.7. More importantly, all morphological classes of LIRGs span a similar range of infrared and optical luminosities. In contrast, at lower redshift, the fraction of spirals decreases and can account for just one third of LIRGs. Furthermore, spirals also appear to be slightly fainter than corresponding peculiar/irregular galaxies.

The local sample used so far to establish this morphological evolution trend is still small. Ishida (2004) performed such a morphological classification for a low redshift sample with 56 LIRGs drawn from the *IRAS* Bright Galaxy Sample (Soifer et al. 1987). Clearly a larger sample is desirable to firmly establish the local statistics. We assemble such a sample by cross-correlating the *IRAS* source catalogue and the Data Release 2 (DR2) of the Sloan Digital Sky Survey (SDSS, see below). Our LIRG sample includes 159 objects with redshift $z \lesssim 0.1$; each has color images from the SDSS. Due to the low-redshift of our objects, the linear physical resolution of the SDSS images is comparable to that achieved for the high redshift objects observed with ACS on board the HST (Melbourne et al. 2005). Therefore comparisons in the morphology of our local sample and those at intermediate redshift can provide a clear picture for the morphological evolution of LIRGs since $z \sim 1$. The outline of the paper is as follows. In §2 we describe our local LIRG sample and in §3 we discuss the morphological classification. In §4 we summarize and discuss our results. Throughout this paper we adopt a cosmology with a matter density parameter $\Omega_m = 0.3$, a cosmological constant $\Omega_\Lambda = 0.7$ and a Hubble constant of $H_0 = 70 \text{ km s}^{-1} \text{Mpc}^{-1}$.

2. The Samples

Our sample LIRGs are drawn from the LIRG catalog of Cao et al. (2005), who carried out a cross-correlation study of the *IRAS* point source catalogue (PSC) and faint source catalogue (FSC) (Moshir et al. 1992) with DR2 of the SDSS (Abazajian et al. 2004). The total number of LIRGs identified with high reliability from FSC is 908. The *IRAS* survey covers all sky while the DR2 covers only 2627 square degree of sky at a (Petrosian) magnitude limit of 17.77 mag in the r band. Note that the catalog of Cao et al. (2005) may miss some local LIRGs that are too faint (for example, due to heavy dust extinctions) to be included in the SDSS (for detail see Cao et al. 2005).

As pointed out by Fukugita et al. (2004), reliable visual morphological classification

can be performed only for SDSS galaxies brighter than $r = 15.9$ mag after correcting for the Galactic extinction (Schlegel et al. 1998). We therefore restrict our sample LIRGs to be brighter than 15.9 mag in the r -band. In addition, we selected only the LIRGs from the FSC LIRGs sample of Cao et al. (2005) with $IRAS$ $60\mu\text{m}$ flux greater than 0.3 Jy to guarantee the sample completeness. This and the magnitude limit reduces the total number of LIRGs for analysis from 908 to 159.

The r -band magnitude, redshift and infrared luminosity distributions of the sample are shown in Fig. 1. It is clear from Fig. 1 that our sample LIRGs have $z \lesssim 0.1$, and most of them are in the redshift range of $0.04 < z < 0.07$. The LIRG sample in this redshift range is just what is needed to extend the analysis for the evolution of LIRGs based on CDFS and GOODS-N since $z \sim 1$ to the local universe. As can be seen from the bottom left panel of Fig. 1, most of our LIRGs have infrared luminosity smaller than $\sim 6 \times 10^{11}L_\odot$.

LIRGs are undergoing high star formation activities, and so the stellar population in these galaxies is a mix of young and old stars. The stellar mass for the old (evolved) stellar population is estimated based on the SDSS photometric data following Bell et al. (2003):

$$\log(M_*/M_\odot) = -0.4(M_{r,\text{AB}} - 4.67) + [a_r + b_r \times (g - r)_{\text{AB}} + 0.15], \quad (1)$$

where the $M_{r,\text{AB}}$ is the r -band absolute magnitude, $(g - r)_{\text{AB}}$ is the rest-frame color in the AB magnitude system. The term 4.67 is the absolute magnitude of the Sun in the SDSS r_{AB} band. The photometric k -correction is calculated using the method of Blanton et al. (2003, `kcorrect v4_1_4`). The coefficients a_r and b_r are taken from Table 7 of Bell et al. (2003). Note that throughout this paper, a Salpeter (1955) stellar initial mass function (IMF) is used, which gives a stellar mass that is 0.15 dex higher (the last term in Eq. 1) than that in Bell et al. (2003) where a modified “diet” Salpeter stellar IMF is used.

The bottom right panel of Fig. 1 shows the stellar mass distribution of 159 local LIRGs. We can see from Fig. 1 that the stellar mass of the old stellar population for most local LIRGs is in the range of $2.5 \times 10^{10} M_\odot$ to $4 \times 10^{11} L_\odot$, indicating most local LIRGs are intermediate mass galaxies, within a factor of few of the stellar mass in the Milky Way.

The star formation rate (SFR) of LIRGs is derived following Kennicutt (1998)

$$\text{SFR} = 4.5 M_\odot \text{ yr}^{-1} \frac{L(8 - 1000\mu\text{m})}{10^{44} \text{ erg s}^{-1}}. \quad (2)$$

The top left panel of Fig. 1 shows the distribution of SFR for our LIRGs sample. In order to estimate the stellar mass assembled during the current starburst phase, we first estimate the CO luminosity using the correlation between the CO luminosity and the infrared luminosity obtained by Gao & Solomon (2004a),

$$\log L_{\text{IR}} = 1.25 \log L'_{\text{CO}} - 0.85, \quad (3)$$

and then obtain the molecular hydrogen mass using the relation

$$M(H_2) = \alpha L'_{\text{CO}} \quad (4)$$

(Gao & Solomon 2004b; Solomon & Bout 2005), where we take α as $4.78 M_{\odot} (\text{K km s}^{-1} \text{ pc}^2)^{-1}$, the approximate value for the Milky Way. Note that the adopted conversion factor α may overestimate the molecular gas mass by a factor of few for interacting/merging LIRGs (Solomon & Bout 2005).

3. Morphological Classifications

To perform morphological classification, color images are produced for all 159 sample LIRGs by combining three color (g , r , i) images using the method of Lupton et al. (2004)¹. We perform morphological classification visually using primarily the r -band images; color images are also used as cross-checks, as in Zheng et al. (2004) and Melbourne et al. (2005). To identify bars in spirals, we use both visual classification and quantitative isophotal analysis (see below). In order to compare the morphology of local LIRGs and those intermediate redshift LIRGs, we adopt the same classification scheme as Melbourne et al. (2005), who divided galaxies into peculiars (interacting and merging), spirals (including barred and non-barred, face-on and edge-on spirals), compact galaxies and elliptical galaxies. However, we found no early type galaxies in our sample, so our objects fall into only three categories.

In practice, we perform classifications as follows. First, we select isolated compact galaxies using the criterion that their half-light radii must be smaller than 3 kpc. The half-light radius is taken to be the r -band Petrosian radius R_{50} , within which half of the r -band Petrosian luminosity is enclosed. There are 20 isolated compact galaxies in our LIRG sample. For the remaining 139 LIRGs, we carry out the morphological classifications visually. The normal spirals have symmetric shape, obvious disk and bulge components and exhibit no disturbed spiral arms. The peculiar galaxy type is characterized by irregular, asymmetric shape and show clear interacting/merging sign or merger relics, such as tidal features. Reliable visual identification of bars can only be done for low-inclination spiral with inclination angle $i < 60^{\circ}$ ($i = 90^{\circ}$ means edge-on). In addition, only strong/obvious bar can be identified with confidence. To further test the reliability of visual bar identification, we also used changes of isophote shapes in the r -band as well as the color images to identify bars (e.g. Jogee et al. 2004; Zheng et al. 2005). The isophote method relies on the fact that at the end of strong bars, there are often rapid changes in position angles and ellipticities.

¹All the images are available at <http://www.jb.man.ac.uk/~smao/LIRG.html>

This approach identified nearly the same barred spirals as the visual search, so we believe our classification of barred galaxies is reliable.

4. Results and Discussions

Out of the 159 sample LIRGs, as discussed above, 20 LIRGs in our sample are classified as isolated compact category according to the criterion of their half-light radius being smaller than 3 kpc. 76 (48%) can be unambiguously classified as interacting/merging galaxies or merger remnants with obvious merger relics. There are an additional 9 objects which show signs of possible interacting or relics of merger. If we add them into the interacting/merging class, the total fraction can be as high as $\sim 52\%$. This fraction is still significantly smaller than that in ULIRGs where almost all are merging/interacting systems. For the remaining LIRGs, 63 (40%) are classified as normal spirals, of which 11 have high inclination angles ($i > 60^\circ$) and hence difficult to perform further bar classification. For the remaining 52 spirals with low inclination angles, 39 (75%) show clear strong bars. This large fraction of barred spirals indicates that bars play an important role in triggering the intense star formation activities in the LIRGs.

Fig. 2 shows three examples for each category. The first and second columns of Fig. 2 show the normal spirals and barred spirals respectively. Clearly some barred spirals have close companions (at least in projection). It is possible that such minor tidal interactions produce both the bar and the symmetric spiral arms, as well as provide the perturbations to channel the gas to the central regions. The third and fourth columns of Fig. 2 show the interacting and merging LIRGs, which exhibit all possible interacting/merging stages, such as interacting pair galaxies, multi-merging groups of galaxies, mergers with two close nuclei, and galaxies with a single nucleus but with merger relics. The compact class of LIRGs is shown in the last column of Fig. 2. They are on average at smaller redshift than the whole sample. These objects share the property of compact sizes, but their morphologies are diverse, from spirals with clear symmetric arms to merging galaxies with tidal features, implying that they may not have a homogeneous physical origin. From the spectroscopic information (Brinchmann et al. 2004), the active galactic nuclei (AGN) fraction in the compact category is not much higher than other classes of LIRGs. Therefore, AGNs are unlikely to be the reason for their compact morphology.

Our morphological classifications for local LIRGs are plotted in Fig. 3 together with the corresponding results from intermediate redshift ($0.1 < z < 1$) taken from Table 1 of Melbourne et al. (2005) based on GOODS-N. Our results are consistent with the extrapolation of theirs to the local universe. These results clearly indicate that the fraction of

interacting/merging galaxies increases from about $\sim 30\%$ at $z \sim 1$ to about 50% at $z \sim 0$. On the other hand, the fraction of spirals decreases from roughly 50% to 40% .

Fig. 4 shows the distribution of infrared luminosity, stellar mass and estimated molecular gas mass for each category. Table 1 lists the number of objects for each morphological class in different luminosity ranges. From Table 1 (and Fig. 4), it is clear that the fraction of interacting/merging LIRGs changes from 40% to 89% when the infrared luminosity increases from $10^{11}L_\odot$ to larger than $4 \times 10^{11}L_\odot$. In contrast, there are no spirals with infrared luminosity larger than $4 \times 10^{11}L_\odot$, implying that they have lower infrared luminosities than interacting/merging LIRGs. The latter dominates in number at higher infrared luminosity, just as in ULIRGs. This result is consistent with that from a deep wide-field survey for LIRGs by Ishida (2004).

The middle column in Fig. 4 illustrates the stellar mass distribution for all local LIRGs. Although the distributions differ in shape for different morphological types, the median stellar mass is almost the same for normal disk galaxies and interacting/merging system; only the compact galaxies have a lower median stellar mass. The stellar masses of the local LIRGs fall into the intermediate mass ranges. This can also be seen in their velocity dispersions. 152 of our galaxies have velocity dispersions available². All types of galaxies have similar ranges of velocity dispersions, except that the velocity dispersions for several objects in the peculiar class exceed 300 km s^{-1} . The median velocity dispersion is $\sim 150 \text{ km s}^{-1}$, similar to the velocity dispersion ($\log \sigma_* = 2.220$) for an L^* galaxy (see Table 1 Bernardi et al. 2005).

The molecular gas mass for each category is also shown in the last column of Fig. 4. Comparing with the middle column, one can see that the normal disk galaxies and interacting/merging system have molecular gas mass $\sim 15\%$ of their stellar mass, which is much higher than the molecular gas fraction of the Milky Way (just a few percent). The median estimated molecular gas mass is about $\sim 1.6 \times 10^{10}M_\odot$. At the current star formation rate (~ 17 to $170 M_\odot \text{ yr}^{-1}$) in the LIRGs (see below), the reservoir of molecular gas M_{H_2} will be consumed in less than 1 Gyr, much shorter than the Hubble time. This may also explain why their number density is low, as their life time is too short to be readily observable.

Fig. 5 shows the star formation rate vs. the stellar mass. We also estimated the average star formation rate, $\langle \text{SFR} \rangle$, following Bell et al. (2005), by dividing the stellar mass by the age of the stellar population, t_{SF} . We assume t_{SF} to be 12 Gyr, which is appropriate if star formation started at $z \sim 4$. Taking into account 30% of the returned mass through stellar winds from stars within 12 Gyr for a Salpeter stellar IMF (Boselli et al. 2001), we have $\langle \text{SFR} \rangle \approx M_*/(0.7t_{\text{SF}})$. As discussed by Bell et al. (2005), t_{SF} is uncertain,

²<http://www.mpa-garching.mpg.de/SDSS/>

nevertheless $\langle \text{SFR} \rangle$ gives a rough indication of the star formation activity in the past. In Fig. 5, almost all LIRGs are located above the horizontal line corresponding to the case where the current SFR is equal to the past average SFR, implying that almost all the local LIRGs are, unsurprisingly, undergoing an elevated episode of star formation. Fig. 5 also shows that interacting/merging galaxies tend to have higher values $\text{SFR}/\langle \text{SFR} \rangle$ compared with other types of LIRGs (spirals and compact galaxies). Furthermore, we can also see that most local LIRGs, even the compact LIRGs, have intermediate stellar mass (indicated by the shaded region), as we argued above.

Recent study on the evolution of the comoving infrared luminosity density of the $24\mu\text{m}$ bright sources observed with the *Spitzer* MIPS in the CDFS shows that LIRGs can account for a significant fraction of the source counts at $0.5 < z < 1$. Their stellar masses cover a wide range, from a few times $10^9 M_\odot$ to a few times $10^{11} M_\odot$ (Bell et al. 2005; Le Floc'h et al. 2005). Deep *Spitzer* MIPS observations (Reddy et al. 2006) find a similar stellar mass range for LIRGs at $1.5 < z < 2.5$ ($2 \times 10^9 M_\odot$ to $5 \times 10^{11} M_\odot$). Compared with high redshift LIRGs, local LIRGs have a narrower range but higher values of stellar masses ($> 2.5 \times 10^{10} M_\odot$).

Taken together the morphological evolution of LIRGs shown in Fig. 3 and the high fraction of barred spirals, it appears that most LIRGs are either major mergers between gas-rich spirals enroute to the formation of intermediate mass ellipticals, or disk galaxies undergoing a major episode of star formation associated with bars. In contrast, high redshift LIRGs are much more abundant and span a broader stellar mass range. One crucial difference between low and high redshifts LIRGs is the available gas reservoir for star formation. At high redshift, the gas reservoir is much higher, so the LIRG phase can occur in a variety of environments, perhaps ranging from the assembly of dwarf galaxies, bulges and cores of ellipticals, resulting in a large range of stellar masses. In the local universe, most of the gas has already been turned into stars, and hence gas-rich galaxies are rare. Either major mergers and/or bars are required to bring the gas into the centers of galaxies and trigger the high star formation rate seen in LIRGs (see Jogee, Scoville & Kenney 2005 for an excellent discussion).

While the local LIRGs are rare, and can just account for about 5% of the total infrared energy from galaxies (Le Floc'h et al. 2005), nevertheless, their proximity renders detailed study of these objects easier than their much more abundant high-redshift counterparts. The understanding of these objects may provide important insights into the physical mechanism that drives the star formation process in the local universe, and how disks and spheroidals are assembled both locally and in the past.

We thank X. Z. Zheng, C. N. Hao and Z. L. Zou for advice and helpful discussions.

This project is supported by NSF of China No.10333060, No.10273012, No.10473013. XYX acknowledges financial support by the visitor's grant at Jodrell Bank. SM thanks the Chinese Academy of Sciences and Tianjin Normal University for travel support. Funding for the creation and distribution of the SDSS Archive has been provided by the Alfred P. Sloan Foundation, the Participating Institutions, the National Aeronautics and Space Administration, the National Science Foundation, the U.S. Department of Energy, the Japanese Monbukagakusho, and the Max Planck Society. The SDSS Web site is <http://www.sdss.org/>. The SDSS is managed by the Astrophysical Research Consortium (ARC) for the Participating Institutions. The Participating Institutions are The University of Chicago, Fermilab, the Institute for Advanced Study, the Japan Participation Group, The Johns Hopkins University, the Korean Scientist Group, Los Alamos National Laboratory, the Max-Planck-Institute for Astronomy (MPIA), the Max-Planck-Institute for Astrophysics (MPA), New Mexico State University, University of Pittsburgh, Princeton University, the United States Naval Observatory, and the University of Washington.

REFERENCES

- Abazajian, K., et al. 2004, AJ, 128, 502
- Bell, E. F., McIntosh, D. H., Katz, N. & Weinberg, M. D. 2003, ApJS, 149, 289
- Bell, E. F., et al. 2005, ApJ, 625, 23
- Bernardi, M., Sheth, R. K., Nichol, R. C., Schneider, D. P., & Brinkmann, J. 2005, AJ, 129, 61
- Blanton, M. R., et al. 2003, AJ, 125, 2348
- Brinchmann, J., Charlot, S., White, S. D. M., Tromonti, C., Kauffmann, G., Heckmann, T., & Brinkmann, J. 2004, MNRAS, 351, 1151
- Boselli, A., Gavazzi, G., Donas, J. & Scoggio, M. 2001, AJ, 121, 753
- Cao, C., Wu, H. , Wang, J. L., Hao, C. N., Deng, Z. G., Xia, X. Y., & Zou, Z. L. 2006, ChJAA, in press (astro-ph/0511097)
- Cowie, L. L., Songaila, A., Hu, E. M., & Cohen, J. G. 1996, AJ, 112, 839
- Cui, J., Xia, X. Y., Deng, Z. G., Mao, S., & Zou, Z. L. 2001, AJ, 122, 63
- Dickinson, M., Pavovich, C., Ferguson, H. C., & Budavári, T. 2003, ApJ, 587, 25
- Elbaz, D. 2005, SSRv, 119, 93
- Fukugita, M., Nakamura, O., Turner, E. L., Helmboldt, J., & Nichol, R. C. 2004, ApJ, 601, L127
- Gao, Y., & Solomon, P. M. 2004a, ApJS, 152, 63
- Gao, Y., & Solomon, P. M. 2004b, ApJ, 606, 271
- Genzel, R., Tacconi, L. J., Rigopoulou, D., Lutz, D., & Tecza, M. 2001, ApJ, 563, 527
- Hammer, F., Flore, H., Elbaz, D., Zheng, X. Z., Liang, Y. C., & Cesarsky, C. 2005, A&A, 430, 115
- Ishida, C. M. 2004, Ph.D. Thesis, University of Hawaii
- Jogee, S., et al. 2004, ApJ, 615, L105
- Jogee, S., Scoville, N., & Kenney, J. D. P. 2005, ApJ, 630, 837

- Kennicutt, R. C. 1998, *ARA&A*, 36, 189
- Le Floc'h, et al. 2005, *ApJ*, 632, 169
- Lonsdale, C., Farrah, D., & Smith, H. 2006, in “Astrophysics Update 2 - topical and timely reviews on astronomy and astrophysics”, Ed. John W. Mason (Springer Verlag) (astro-ph/0603031)
- Lupton, R., Blanton, M.R., Fekete, G., Hogg, D.W., O'Mullane, W., Szalay, A. & Wherry, N. 2004, *PASP*, 116, 133
- Melbourne, J., Koo, D. C., & Le Floc'h, E. 2005, *ApJ*, 632, L65
- Moshir M., Kopan G., Conrow J., et al. 1992. Explanatory Supplement to the *IRAS* Faint Source Survey, Version 2, JPL D-10015 8/92, Pasadena: JPL
- Reddy, N. A., Steldel, C. C., Fadda, D., Yan, L., Pettini, M., Shapley, A. E., Erb, D. K., & Adelberger, K. L. 2006, *ApJ*, in press (astro-ph/0602596)
- Salpeter, E. 1995, *ApJ*, 121, 161
- Sanders, B. T., & Mirabel, I. F., 1996, *ARA&A*, 34, 749
- Schlegel, D. J., Finkbeiner, D. P., & Davis, M. 1998, *ApJ*, 500, 525
- Solomon, P. M., & vanden Bout, P. A. 2005, *ARA&A*, 43, 677
- Soifer, B. T., Sanders, D. B., Madore, B. F., Neugebauer, G., Danielson, G. E., Elias, J. H., Lonsdale, C. J., & Rice, W. L. 1987, *ApJ*, 320, 238
- Tacconi, L. J., et al. 2006, in press (astro-ph/0511319)
- Werner, M. W., et al. 2004, *ApJS*, 154, 1
- Zheng, X. Z., Hammer, F., Flores, H., Assémat, F., & Pelat, D. 2004, *A&A*, 421, 847
- Zheng, X. Z., Hammer, F., Flores, H., Assémat, F., & Rawat, A. 2005, *A&A*, 435, 507

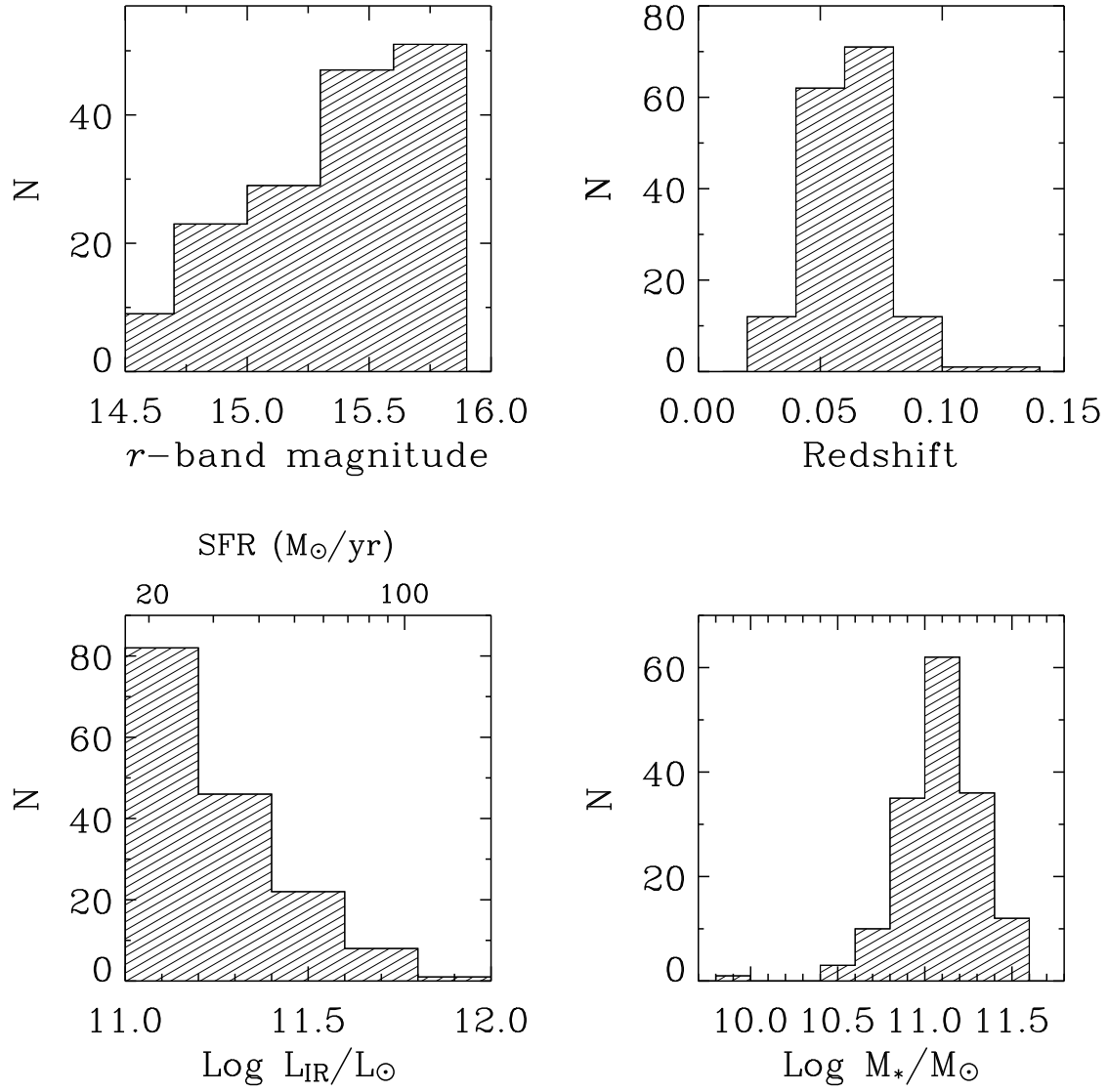


Fig. 1.— r -band magnitude, redshift, infrared luminosity (SFR) and stellar mass distributions for our luminous infrared galaxy (LIRG) sample.

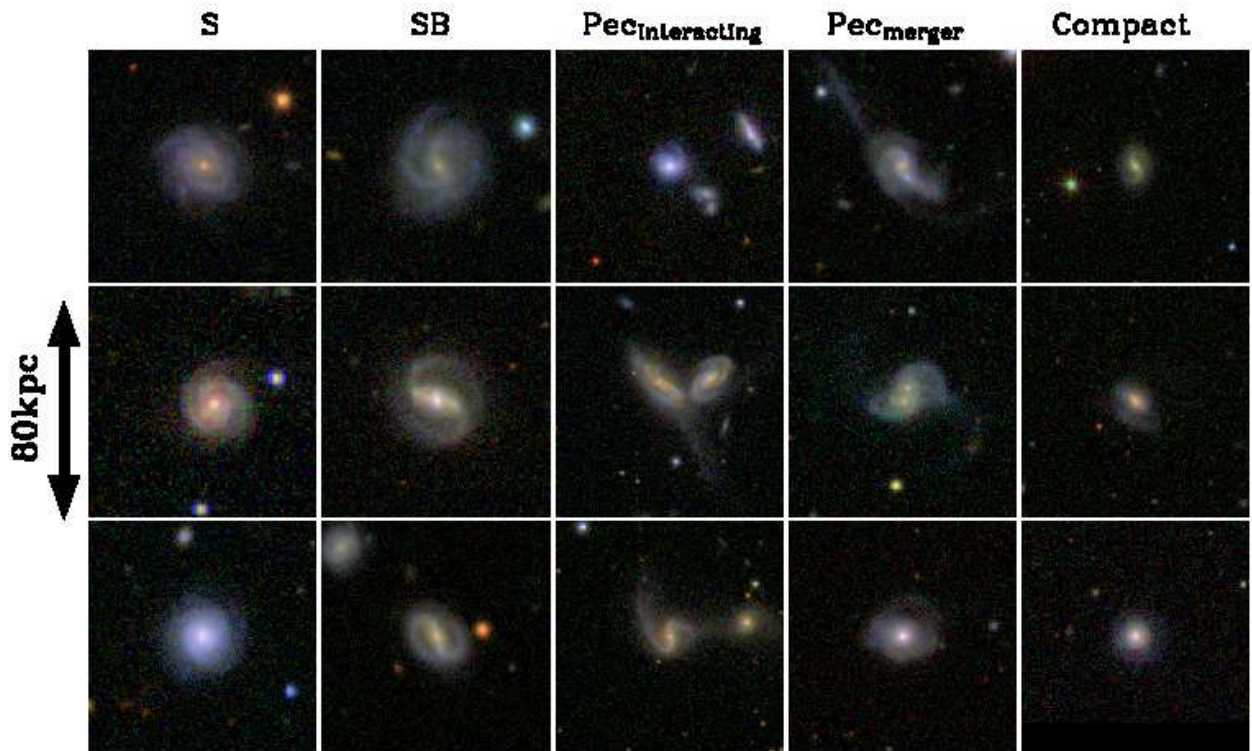


Fig. 2.— Three color images of 15 galaxies. Each color image is produced by combining three (g, r, i) SDSS images using the method of Lupton et al. (2004). The images are grouped into five columns: S - nonbarred spiral, SB - barred galaxies, Pec_{Interacting} - interacting galaxies, Pec_{merger} - merging galaxies, and Compact galaxies. Three examples are shown for each morphology class.

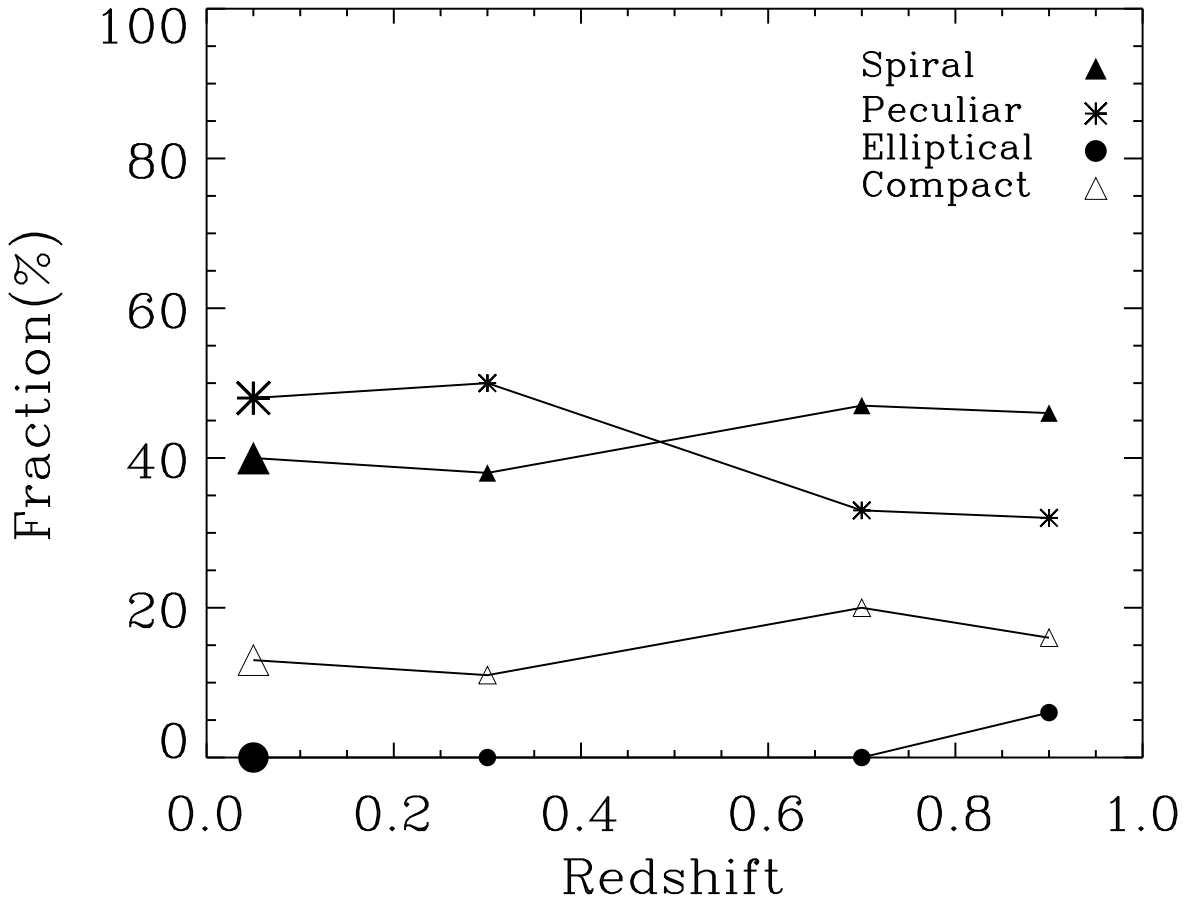


Fig. 3.— Morphological classification of LIRGs in the local universe (at $z \sim 0.05$, large symbols) compared with those of Melbourne et al. (small symbol) at intermediate redshift. The spiral category includes barred, nonbarred and highly-inclined spirals. In the local sample, there are no ellipticals. The redshift shown is the median value of galaxy redshifts in each bin.

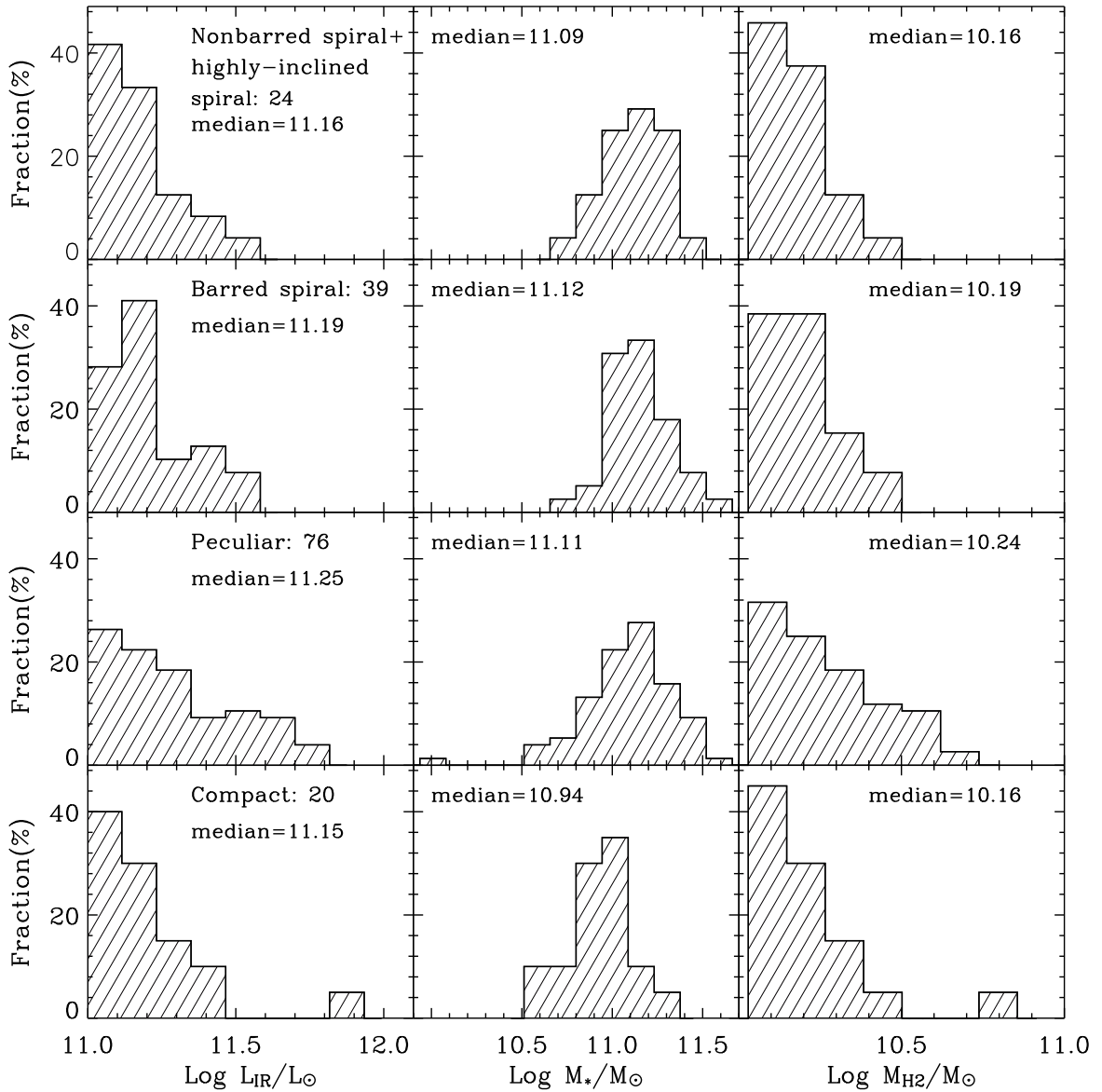


Fig. 4.— Distribution of infrared luminosity, stellar mass and the molecular gas mass for different morphological classes.

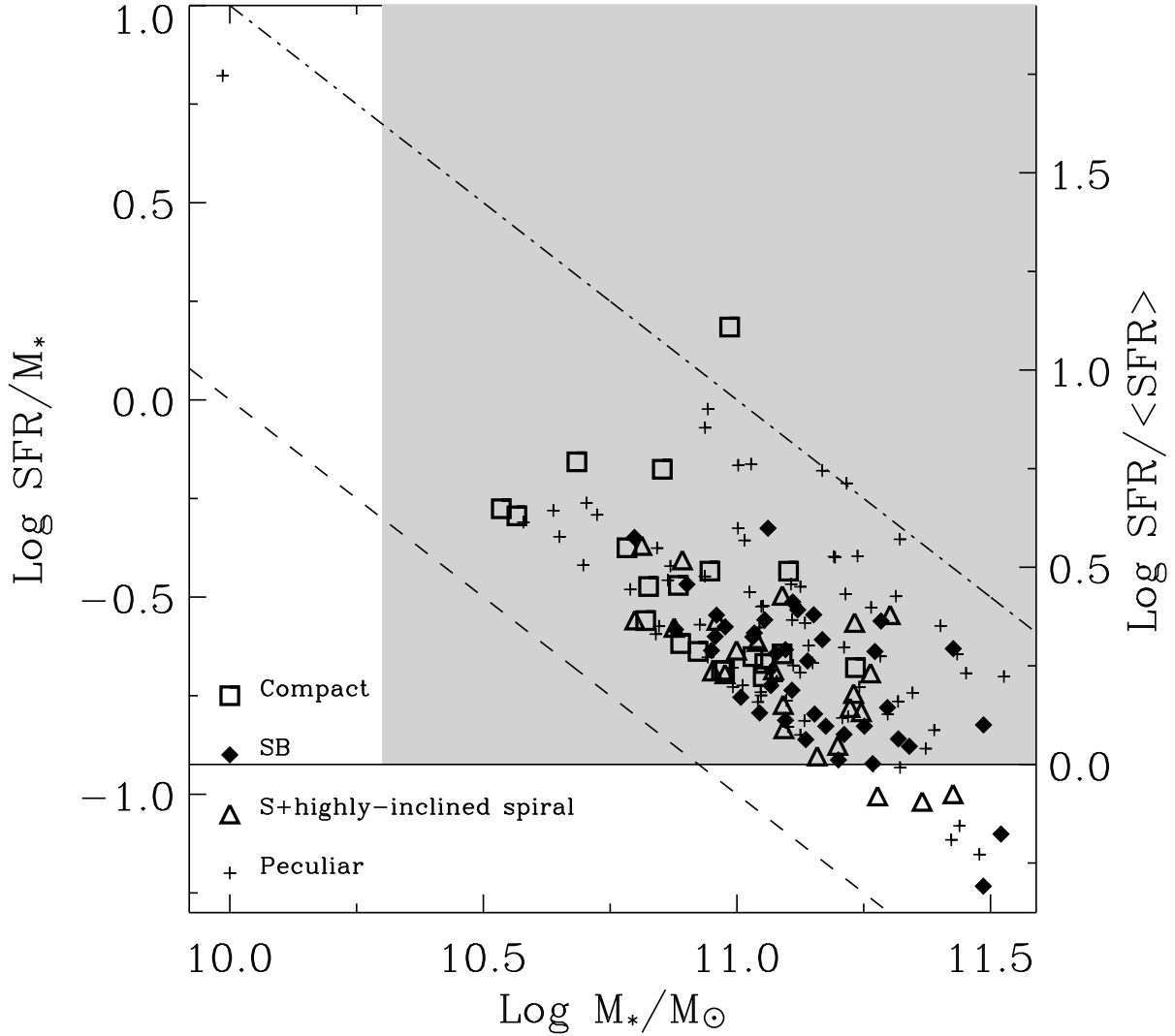


Fig. 5.— star formation rate per Gyr per unit stellar mass as a function of stellar mass for each category of LIRGs. The dashed and dot-dashed lines denote a SFR of 10 and 100 $M_\odot \text{ yr}^{-1}$ respectively, while the horizontal line is for a constant SFR as a function of time. The birthrate parameter (current SFR divided by the past average SFR) is plotted on the right axis. The shaded region indicates the rough range of intermediate mass galaxies.

Table 1. Morphology classification

	11 < $\log(L_{\text{IR}}/L_{\odot})$		11 < $\log(L_{\text{IR}}/L_{\odot}) < 11.3$		11.3 < $\log(L_{\text{IR}}/L_{\odot}) < 11.6$		11.6 < $\log(L_{\text{IR}}/L_{\odot})$	
	N	%	N	%	N	%	N	%
Total	159	100	111	100	39	100	9	100
Nonbarred spiral	13	8	10	9	3	8	0	0
Barred spiral	39	25	30	27	9	23	0	0
Highly-inclined	11	7	10	9	1	3	0	0
Peculiar	76	48	45	41	23	59	8	89
Compact	20	13	16	14	3	8	1	11